Epilepsy & Behavior 71 (2017) 226–237

Contents lists available at ScienceDirect

Epilepsy & Behavior

journal homepage: www.elsevier.com/locate/yebeh

Overexpression of the immediate-early genes Egr1, Egr2, and Egr3 in two strains of rodents susceptible to audiogenic seizures

D. López-López [a,b], R. Gómez-Nieto [a,b,c], M.J. Herrero-Turrión [a], N. García-Cairasco [d], D. Sánchez-Benito [a,b], M.D. Ludeña [c], D.E. López [a,b,c,*]

[a] Institute for Neuroscience of Castilla y León (INCyL), University of Salamanca, Salamanca, Spain
[b] Salamanca Institute for Biomedical Research (IBSAL), Spain
[c] Department of Cell Biology and Pathology, School of Medicine, University of Salamanca, Salamanca, Spain
[d] Physiology Department, Ribeirão Preto School of Medicine, University of São Paulo, Ribeirão Preto, Brazil

ARTICLE INFO

Article history:
Revised 10 December 2015
Accepted 12 December 2015
Available online 14 January 2016

Keywords:
Audiogenic epilepsy
Early growth response
GASH:Sal
Seizure-induced transcriptome
Microarray
WAR

ABSTRACT

Genetic animal models of epilepsy are an important tool for further understanding the basic cellular mechanisms underlying epileptogenesis and for developing novel antiepileptic drugs. We conducted a comparative study of gene expression in the inferior colliculus, a nucleus that triggers audiogenic seizures, using two animal models, the Wistar audiogenic rat (WAR) and the genetic audiogenic seizure hamster (GASH:Sal). For this purpose, both models were exposed to high intensity auditory stimulation, and 60 min later, the inferior colliculi were collected. As controls, intact Wistar rats and Syrian hamsters were subjected to stimulation and tissue preparation protocols identical to those performed on the experimental animals. Ribonucleic acid was isolated, and microarray analysis comparing the stimulated Wistar and WAR rats showed that the genomic profile of these animals displayed significant (fold change, $|FC| \geq 2.0$ and $p < 0.05$) upregulation of 38 genes and downregulation of 47 genes. Comparison of gene expression profiles between stimulated control hamsters and stimulated GASH:Sal revealed the upregulation of 10 genes and the downregulation of 5 genes.

Among the common genes that were altered in both models, we identified the zinc finger immediate-early growth response gene *Egr3*. The Egr3 protein is a transcription factor that is induced by distinct stress-elicited factors. Based on immunohistochemistry, this protein was expressed in the cochlear nucleus complex, the inferior colliculus, and the hippocampus of both animal models as well as in lymphoma tumors of the GASH:Sal. Our results support that the overexpression of the *Egr3* gene in both models might contribute to neuronal viability and development of lymphoma in response to stress associated with audiogenic seizures.

This article is part of a Special Issue entitled "Genetic and Reflex Epilepsies, Audiogenic Seizures and Strains: From Experimental Models to the Clinic".

1. Introduction

Epilepsy is a complex neurological disorder in terms of both its etiology and its cognitive, behavioral, electrophysiological, molecular, and cellular pathology [1–3]. Although enormous progress has been made in understanding the etiology of epilepsy, the current knowledge is very limited. The complexity of this neurological disorder requires intense interdisciplinary research. Thus, at the moment, a variety of models are available for exploring different aspects of epilepsy such as in silico [4], in vivo [5], and in vitro [6].

Some in vivo models represent the natural association between genetic predisposition and external events that trigger seizures [7]. Among the most used and well-characterized in vivo genetic models of epilepsy are audiogenic seizures, which are triggered by high intensity acoustic stimulation. The substantial characterization of their neural substrates, as well as their behavioral, cellular, and molecular alterations, combined with pharmacologically- or electrically-induced seizures, potentiates their usefulness in the elucidation of epileptogenesis and preclinical development of new antiepileptic drugs [8,9].

The present study focused on two animal strains that are categorized as audiogenic seizure models, the Wistar audiogenic rat (WAR) and the genetic audiogenic seizure hamster (GASH:Sal).

The WAR is a genetically selected strain susceptible to audiogenic seizures that was inbred at the School of Medicine of Ribeirão Preto (Brazil) beginning in 1990. This strain is a model of audiogenic idiopathic epilepsy that develops tonic–clonic generalized seizures [10,11].

* Corresponding author at: Institute for Neuroscience of Castilla y León (INCyL), Laboratory 12, C/Pintor Fernando Gallego 1, 37007 Salamanca, Spain. Tel.: +34 923294400x1868.
E-mail address: lopezde@usal.es (D.E. López).

http://dx.doi.org/10.1016/j.yebeh.2015.12.020
1525-5050/

The GASH:Sal, a hamster strain developed at the University of Salamanca, exhibits genetic audiogenic epilepsy similar to human tonic–clonic seizures [12]. The GASH:Sal shows an autosomal recessive inheritance for susceptibility to audiogenic seizures, which manifests more severely in young animals; the seizure severity progressively declines with age [13].

Similar to other animal models of audiogenic seizures [14–16], those with brainstem origin occur as a result of intense auditory stimulation [13,17]. Activation of auditory pathways is crucial for expression of the audiogenic seizure phenotype, and the inferior colliculus, in the auditory midbrain, plays a key role in its initiation [15,16]. Thus, bilateral lesions in the central nucleus of the IC permanently block audiogenic seizures [14,18–20], and lesions in the dorsal and external cortices of the IC partially attenuate the audiogenic seizures [14,21].

To find common molecular processes between these two models of audiogenic seizures, we have conducted a comparative analysis of the profiles of gene expression in the inferior colliculus (IC), a nucleus that triggers audiogenic seizures. Of all the possible comparisons, we have selected stimulated controls for comparison with the stimulated audiogenic strains, either GASH:Sal or WAR, to avoid bias related to sound-induced gene expression. Some of the deregulated genes detected via microarray analysis were validated by quantitative reverse transcription real-time PCR (RT-qPCR).

The present study might contribute toward understanding basic mechanisms associating genetic predisposition to epilepsy, early gene expression after seizures, and the recognition of new targets that could be consequently tested in the development of antiepileptic drugs.

Briefly, our results are important for the identification, in this particular case, of early genes induced by seizures and suggest molecular processes with potential implications for human epilepsy.

2. Material and methods

2.1. Experimental animals

A total of 51 animals were used in this study according to the following distribution: 17 male WAR and 6 male control rats (*Rattus norvegicus*, Wistar albino, Charles River Laboratories) at 12 weeks of age and a body weight of approximately 230 g. In the case of the hamsters, we used 12 control Syrian hamsters (*Mesocricetus auratus*) and 16 GASH:Sal at 16 weeks of age, weighing approximately 60 g. The WAR and GASH:Sal animals did not suffer any audiogenic seizure prior to the experiments. All animals were free of ear infection. To rapidly confirm normal hearing, we used the bilateral finger friction test in all cases.

The animals were exposed to auditory stimulation within an acrylic cylinder. The acoustic stimulus was recorded using a high-pass filter (>500 Hz; microphone Bruel & Kjaer #4134 and preamplifier Bruel & Kjaer #2619), digitized above 4 kHz, and reproduced by a computer coupled to an amplifier (Fonestar MA-25T, Revilla de Camargo, Spain) and a tweeter (Beyma T2010, Valencia, Spain) in the upper portion of the arena. The delivered sound was a semirandom acoustic stimulus of 0–18 kHz with an intensity of 115 to 120 dB. For more information see [10,22]. Sixty minutes after the seizures, we harvested the IC for all gene expression analyses. As controls, normal Wistar rats and Syrian hamsters were exposed to the same stimulation according to the identical procedure.

For each gene microarray (Rat Gene 1.0 ST & Microarray MoGene 1.0 ST), the rats or hamsters were randomly divided into four groups, and we used the right and left inferior colliculi from each animal (Table 1). For the transcriptomic analyses, we compared only stimulated Syrian hamsters and stimulated GASH:Sal, using four animals of each strain. For RT-qPCR, 3 to 8 of the replicates from each group were randomly selected and performed in triplicate on two separate occasions for each gene product examined.

Table 1
Number of animals used in this study in the different experimental approaches.

N	Microarray Rat Gene 1.0 ST	RT-qPCR	Histology
Wistar rat	4	3	N/A
Stimulated Wistar rat	3	3	N/A
WAR	6	6	2
Stimulated WAR	7	6	2

N	Microarray MoGene 1.0 ST	RT-qPCR	Histology	Transcriptome
Syrian hamster	6	3 (6 I.C.)	N/A	N/A
Stimulated Syrian hamster	6	3 (6 I.C.)	N/A	4 (7 I.C.)
GASH:Sal	6	4 (8 I.C.)	2	N/A
Stimulated GASH:Sal	6	3 (6 I.C.)	2	4 (8 I.C.)

2.2. Ethics statement

All procedures and experimental protocols were performed according to the guidelines of the European Community's Council Directive (2010/63/CE) and Brazilian legislation for the care and use of laboratory animals.

The experiments were performed at both the Neuroscience Institute of Castilla y León at the University of Salamanca and the Ribeirão Preto School of Medicine at the University of São Paulo, with the approval of the Animal Care and Ethics Committees of those institutions.

2.3. Tissue sampling

After anesthetizing the animals with an overdose of sodium pentobarbital, the IC was isolated, surgically removed, and placed in TRIzol® (Gibco BRL, Gaithersburg, MD, USA) for transcription analysis. For immunohistological studies, the protocols used for tissue preparation, including perfusion of the animals, brain dissection, and tissue slicing, were identical to those used elsewhere [23,24].

2.4. RNA isolation

Total RNA was purified using TRIzol®, followed by further RNA purification using an RNeasy Mini Kit for RNA cleanup (Qiagen Sciences, Germantown, Maryland, USA). Ribonucleic acid quantity and quality were then assessed using an Agilent 2100 Bioanalyzer (Agilent Technologies, Palo Alto, CA, USA) to test the integrity of the 18S and 28S ribosomal RNA (rRNA) bands, and samples displaying an RNA integrity number (RIN) > 8.0 were used.

2.5. Microarray hybridization data analysis: normalization, differential gene expression, and ontological analysis

Microarray analysis was performed at the Cancer Research Center of Salamanca according to standard procedures. Labeling and hybridization were performed according to protocols from Affymetrix. Briefly, 100–300 ng of total RNA was amplified and labeled using the WT Sense Target labeling and control reagents kit (Affymetrix Inc., Santa Clara, CA, USA) and was then hybridized to rat (Gene 1.0 ST Array) or mouse (GeneChip® Mouse Gene ST Array) microarrays, as appropriate. Washing and scanning were performed using the Affymetrix GeneChip system (GeneChip Hybridization Oven 640, GeneChip Fluidics Station 450, and GeneChip Scanner 7G).

Following image analysis, the microarray data were imported into GeneSpring GX7.3 (Agilent Technologies). The robust multiarray analysis (RMA) algorithm [25] was used for background correction and normalization of fluorescent hybridization signals of the microarrays at both the internal (intramicroarrays) and the comparative (intermicroarrays) levels. This algorithm was selected over other

available algorithms such as the MAS5 or MBEI [26] because it was deemed to provide the best precision in signal detection to achieve adequate multiple-chip normalization [27], especially in cases of low-level gene expression [25,28,29], by producing efficient quantile normalization of the distribution of probe intensities from each array in the context of a complete set of arrays.

We used Bioconductor and R as computational tools (www.bioconductor.org) to apply RMA to the dataset of microarray hybridizations including 3 to 6 different biological replicates corresponding to each of the experimental groups in the study (Wistar rat or Syrian hamster control, stimulated Wistar rat or Syrian hamster, WAR or GASH:Sal control, and stimulated WAR or GASH:Sal).

After quantitation of the expression level of each probe set in all analyzed Rat Gene 1.0 ST microarrays, the significance analysis of microarrays (SAM) algorithm [30] was used to identify probe sets displaying significant differential expression when comparing the experimental samples to their controls. This algorithm performs statistical discrimination analysis using permutations to check the stability of variables fulfilling the 'alternative hypothesis'. This method calculates the type I error, or the number of expected false positives, by calculating the false discovery rate (FDR) [31]. In this report, genes displaying an FDR of 6% or less were considered as significant. We selected the genes that vary in a range (fold change, $|FC| \geq 2$) among other genes and used different databases to determine their function.

In the case of the MoGene 1.0 ST microarrays, we compared the experimental groups corresponding to the stimulated hamster control and the stimulated GASH:Sal; all of our samples passed a stringent data quality control test and showed high intragroup homogeneity [32].

Potential differential expression was determined via one-way analysis of variance (ANOVA) (variances not assumed to be equal). Subsequently, an unpaired *t*-test ($p < 0.05$, filtered at 1.5 fold) was performed to search for the genes exhibiting differential expression (the levels in the control samples were considered as the basal levels) [32].

The data obtained and discussed in this publication have been deposited in the NCBI's Gene Expression Omnibus [33] at GEO Series accession numbers GSE74150 (http://www.ncbi.nlm.nih.gov/geo/query/acc.cgi?acc=GSE74150) for the WAR arrays and GSE74043 (http://www.ncbi.nlm.nih.gov/geo/query/acc.cgi?acc=GSE74043) for the GASH:Sal arrays.

Further processing, including functional analysis and overrepresentation calculations based on the Gene Ontology (GO) Annotation Tool and published data from the Database for Annotation, Visualization, and Integrated Discovery, was performed using GeneSpring GX 7.3 and DAVID Bioinformatics Resources 6.7 (http://david.abcc.ncifcrf.gov/) [34].

2.6. Transcriptome of the inferior colliculus, RNASeq library generation, sequencing, and bioinformatic analysis

The analysis was performed using 15 biological samples of the left or right IC, which were obtained from male GASH:Sal and control hamsters (HdsHan®:AURA). Specifically, 8 IC samples were obtained from the controls (4 from the left and 4 from the right IC), and 7 IC samples were obtained from GASH:Sal (4 from the left and 3 from the right IC).

The pool of isolated and precipitated RNAs was generated using 3 samples from each animal type, taking 1 μg of RNA from each animal, and 3 μg of the pooled RNA was used for the creation of RNASeq libraries using the TruSeq RNA Sample Prep Kit v2 (Illumina) after the removal of rRNA. Both obtained libraries were validated using the 2100 Agilent Bioanalyzer and were quantified via RT-qPCR analysis.

Sequencing of both libraries was conducted using an IIx genome analyzer (Illumina) using the single read format, and the sequences that did not meet the purity criteria in the software were discarded. Quality values were associated with a value of 30 or greater on the Phred scale (0–40) for 25066143 reads PF (pass filter) considering a medium length of 76 bp from the controls and 27848979 reads PF considering the same medium length from GASH:Sal.

After quality control, normalization of the libraries, and detection of no significant deviation between the differential expression and the average expression, we began analyzing the great quantity of data obtained. One of the most interesting means of analysis is the examination of the table containing all of the information about the differentially expressed genes. This information not only provides the biological processes, molecular functions, cellular components, and phenotypes associated with many genes according to their annotation but also describes whether the genes are upregulated or downregulated |FC| and whether the results from a statistical perspective were significant (*p* value).

The data obtained and discussed in this publication have also been deposited in the NCBI BioProject at accession number 230618.

2.7. Quantitative reverse transcription real-time PCR (RT-qPCR)

Total RNA (2 μg), reacted with oligo-dT and random hexamer primers, was reverse transcribed into cDNA at 37 °C for 2 h using the First Strand cDNA Synthesis Kit (Promega Corporation, Madison, WI, USA). In all cases, a reverse transcriptase negative control was used to test genomic DNA contamination.

Quantitative RT-qPCR was performed using the SYBR Green method with a 2× Master Mix (Applied Biosystems). Each reaction contained 10 μl of Master Mix, 0.4 μl of each pair of primers, 3 μl of each cDNA sample in a different serial cDNA quantity for each gene, and MilliQ water up to 20 μl. The amplification reaction was performed in an ABI Prism 7000 detection system (Applied Biosystems) under the following conditions: 10 min at 95 °C followed by 40 cycles of 15 s at 95 °C and 1 min at 60 °C depending on each pair of primers. Quantitative reverse transcription real-time PCR experiments were performed in replicates of 3 to 8 samples and conducted in triplicate for each gene product examined. The list of primers used is provided in Table 2. β-actin was used as the housekeeping gene.

To choose the most stable genes as internal references for RT-qPCR data normalization, two candidates [β-actin and glyceraldehyde 3-phosphate dehydrogenase (*Gapdh*)] were selected according to their expression levels detected in the microarray studied. The expression of these two genes was also measured by RT-qPCR. NormFinder software [35] was used to calculate the intra- and intergroup variations in gene expression. Our results indicated that β-actin is the most stable gene, whereas *Gapdh* is less stable (data not shown). Thus, the mean threshold cycle (Ct) value and primer efficiency value of β-actin were used for normalization.

The comparative Ct method was used for presenting quantitative data [36]. Following the removal of outliers [37], raw fluorescence data were used to determine the PCR amplification efficiency (E) according to the formula $E = [10^{(-1/\text{slope})} - 1] * 100$. All amplifications had an E value of 100 ± 10%, and an E value near 100% indicated efficient amplification. The relative gene expression value (FC) for each transcript was calculated according to the formula $2^{-(\Delta Ct\ \text{“condition 1”} - \Delta Ct\ \text{“condition 2”})}$, where "condition 1" corresponds to the experimental sample, "condition 2" to the sample from the control animal, and ΔCt of each "condition" is $Ct_{\text{“experimental gene”}} - Ct_{\text{“endogenous gene”}}$ [36]. The standard error for each relative gene expression value was calculated as a measure of data variation. The significance of the qPCR analysis results was determined using a one-tailed *t*-test for each gene, considering $|FC| > 1$ as significant ($p < 0.05$).

2.8. Immunostaining

The control animals and the animals exposed to auditory stimulation of both species were euthanized with pentobarbital (60 mg/kg) and perfused transcardially with 0.9% saline wash solution followed by 4% paraformaldehyde fixative solution (Table 1). The time between audiogenic stimulation and sacrifice was 60 min. After the fixative perfusion,

Table 2
Oligonucleotide primers employed.

Target protein	GenBank number[a]	Primer forward	cDNA forward[a]	Primer reverse	cDNA reverse[a]	Size of products	E[b]
Egr1	NM_012551.2| *Rattus norvegicus*	CAGC(A/G)GCGC(T/C)TTCAATCCTC	162–181 502–521	GTGGTCAGGTGCTCGTAGGG	202–221 542–561	60	2.04
	XM_005065288.1| *Mesocricetus auratus*		265–284		305–324		
	XM_007636101.1| *Cricetulus griseus*						
Egr2	XM_003515916.1| *Cricetulus griseus*	AGGCCCTTGGATCTCCCATA	31–50	CAGCTGGCACCAGGGTACTG	127–146	116	2.00
	XM_005070807.1|		347–363		443–462		
	XM_005070806.1| *Mesocricetus auratus*		559–575		655–674		
	AB264614.1| *Rattus norvegicus*		27–46		123–142		
Egr3	XM_006252240.1|	CCACAAGCCCTTCCAGTGTC	1198–1217	GTGCGGATGTGAGTGGTGAG	1253–1273	75	1.98
	XM_006252239.1| *Rattus norvegicus*		1019–1038		1074–1094		
	XM_005071015.1|		789–808		844–860		
	XM_005071014.1|		955–975		1010–1026		
	XM_005071013.1|		1154–1173		1209–1225		
	Mesocricetus auratus		780–799		835–855		
	XM_003496195.1| *Cricetulus griseus*						
Gabra4	XM_008770135.1 *Rattus norvegicus*	CACCAT(A/C)AGTGCGGAGTGTC	1276–1295 498–517	ATTTCAAAGGGCAGGCATGA	1327–1346 549–568	71	1.98
	XM_003507783.2		498–517		549–568		
	XM_007634147.1		441–460		492–511		
	XM_007634149.1		441–460		492–511		
	XM_007634150.1		605–624		656–675		
	Cricetulus griseus		441–460		492–511		
	XM_005080795.1		441–460		492–511		
	XM_005080796.1						
	XM_005080797.1 *Mesocricetus auratus*						
Gapdh	NM_017008.4| *Rattus norvegicus*	ACATGCCGCCTGGAGAAACCT	805–824 802–821	GCCCAGGATGCCCTTTAGTGG	874–894 871–891	90	2.00
	NM_001244854.2| *Cricetulus griseus*						
β-actin	XM_006248886.1| XM_006248885.1| *Rattus norvegicus*	AGCCATGTACGTAGCCATCC	240–259 415–434	ACCCTCATAGATGGGCACAG	335–354 510–529	115	2.03
	XM_007648665.1| *Cricetulus griseus*		489–506 390–407		584–602 485–503		
	NM_001281595.1| *Mesocricetus auratus*						

[a] The primer location in the corresponding GenBank sequences of rat and hamster origin is indicated.
[b] qPCR primer efficiency (E) was calculated according to the following equation: $E = 10^{(-1/\text{slope})}$.

the brains were removed from the skulls and cryoprotected for 48 h at 4 °C in 30% sucrose in phosphate buffer (PB). Coronal brain sections at 40-μm thickness were generated using a freezing sliding microtome. All sections were processed for immunohistochemistry using similar procedures to those used in our previous studies of rats [24] and hamsters [23]. Briefly, the sections were washed and incubated in a rabbit anti-EGR3 primary antibody solution (1:500, #HPA006206, Sigma-Aldrich) diluted in TBS (Tris-buffered saline) for 24 h at 4 °C. The tissue was then washed and incubated with a goat biotinylated secondary antibody anti-rabbit (1:200, #BA-1000, Vector Labs) for 2 h at room temperature and finally visualized with the avidin–biotin–peroxidase complex procedure (Vectastain, Vector Labs) and histochemistry for peroxidase without heavy metal intensification. For each brain, all sections were mounted on slides, dehydrated, and coverslipped. Brain specimens taken from control animals, as well as from WAR and GASH:Sal animals, were processed simultaneously using the same batch of solutions and incubation times in order to minimize the variability in the visualization of immunoreactivity and DAB reaction product. For immunolocalization of markers in the lymphoma-derived tissue samples, the fixed tissues were processed in a commercial histological processor (Technicon, Assens Llofriu, Madrid, Spain), and the resulting paraffin blocks were cut into 3-μm sections. We used a Bond Polymer Refine Detection system (DS9800, Vision BioSystems, Newcastle, UK) (Leica Bond III), which included a polymeric horseradish peroxidase (HRP)-linked antibody for the detection of the secondary antibody, according to the instructions of the manufacturer using the same concentration as cited above.

The primary antibody used was anti-Egr3 (1:500, #HPA006206, Sigma-Aldrich), a polyclonal antibody generated in rabbits against the recombinant early growth response 3 protein epitope signature tag (PrEST) (see details in the manufacturer's technical information).

Negative controls were not treated with primary antibodies, and this resulted in the complete absence of immunolabeling.

The histological sections were thoroughly examined under a microscope (DMBL, Leica), and images were captured using a digital camera (DP50, Olympus) adapted to the microscope.

3. Results

3.1. Microarray analysis

3.1.1. Gene expression arrays of the IC in the control vs. GASH:Sal hamsters after acoustic stimulation

From the full list of genetic analyses obtained from the MoGene 1.0 ST expression arrays of all samples, the analysis of sound-stimulated control hamsters and GASH:Sal was composed of 28,814 entries (26,293 of which were identifiable). The differences between the stimulated controls and stimulated GASH:Sal were analyzed. We identified a total of 82 genes that changed in expression when comparing stimulated controls to stimulated GASH:Sal (see complete list of differentially

expressed genes in Supplemental File 1). Of these 82 genes, we specifically identified 15 genes showing significant fold change (|FC| ≥ 1.5) differences in gene expression. Thus, we found upregulation of 10 genes and downregulation of 5 genes in the stimulated GASH:Sal compared to stimulated control hamsters.

No relationships at the metabolic, structural, or functional level among the 15 genes were observed. Most of the genes were transcription factors (early growth response 2 [*Egr2*], early growth response 3 [*Egr3*], neuronal PAS domain protein 4 [*Npas4*], RAS protein-specific guanine nucleotide-releasing factor 2 [*Rasgrf2*], sterile alpha motif domain-containing 9-like [*Samd9l*]), some of which were related to signaling pathways associated with Rho or Ras proteins (*Rasgrf2*, *Samd9l*). There were also genes related to calcium ion metabolism (ATPase, Ca^{++} transporting, ubiquitous [*Atp2a3*], triadin [*Trdn*]), epigenesis (jumonji, AT-rich interactive domain 1D [*Jarid1d*], ubiquitously transcribed tetratricopeptide repeat gene, Y chromosome [*Uty*]), translation processes (prostaglandin E synthase 3 (cytosolic)-like [Ptges3l]), or several biological processes (ADP-ribosylation factor-like 15 [*Arl15*], calcyclin-binding protein [*Cacybp*], cyclic nucleotide-binding domain-containing 1 [*Cnbd1*]). Interestingly, two of the genes encode transcription factors that belong to the family of early growth response genes, *Egr2* and *Egr3*. The Gene Ontology (GO) annotations related to those genes include sequence-specific DNA binding transcription factor activity and transcription regulatory region DNA binding.

The functional analysis and overrepresentation calculations based on the GO Annotation Tool are shown in Fig. 1A.

3.1.2. Gene expression arrays of the IC in the Wistar vs. WAR rats after acoustic stimulation

Analysis of the differential expression between samples of the IC from stimulated Wistar and WAR rats provided a list of 297 genes. We reduced that list by choosing the most representative genes according to a cutoff absolute fold change of 2 or greater (|FC| ≥ 2).

Comparative analysis of the microarray results between sound-stimulated Wistar and WAR rats showed that the genomic profile of these animals was significantly affected (displaying a |FC| ≥ 2 and $p < 0.05$) in 39 upregulated genes and 32 downregulated genes.

To enhance the biological interpretation of the differentially expressed genes from our microarray studies, we determined whether any of the biological processes or molecular functions were overrepresented among the differentially expressed genes. The functional interpretation of the experimental data in the rat microarrays was performed using the GO

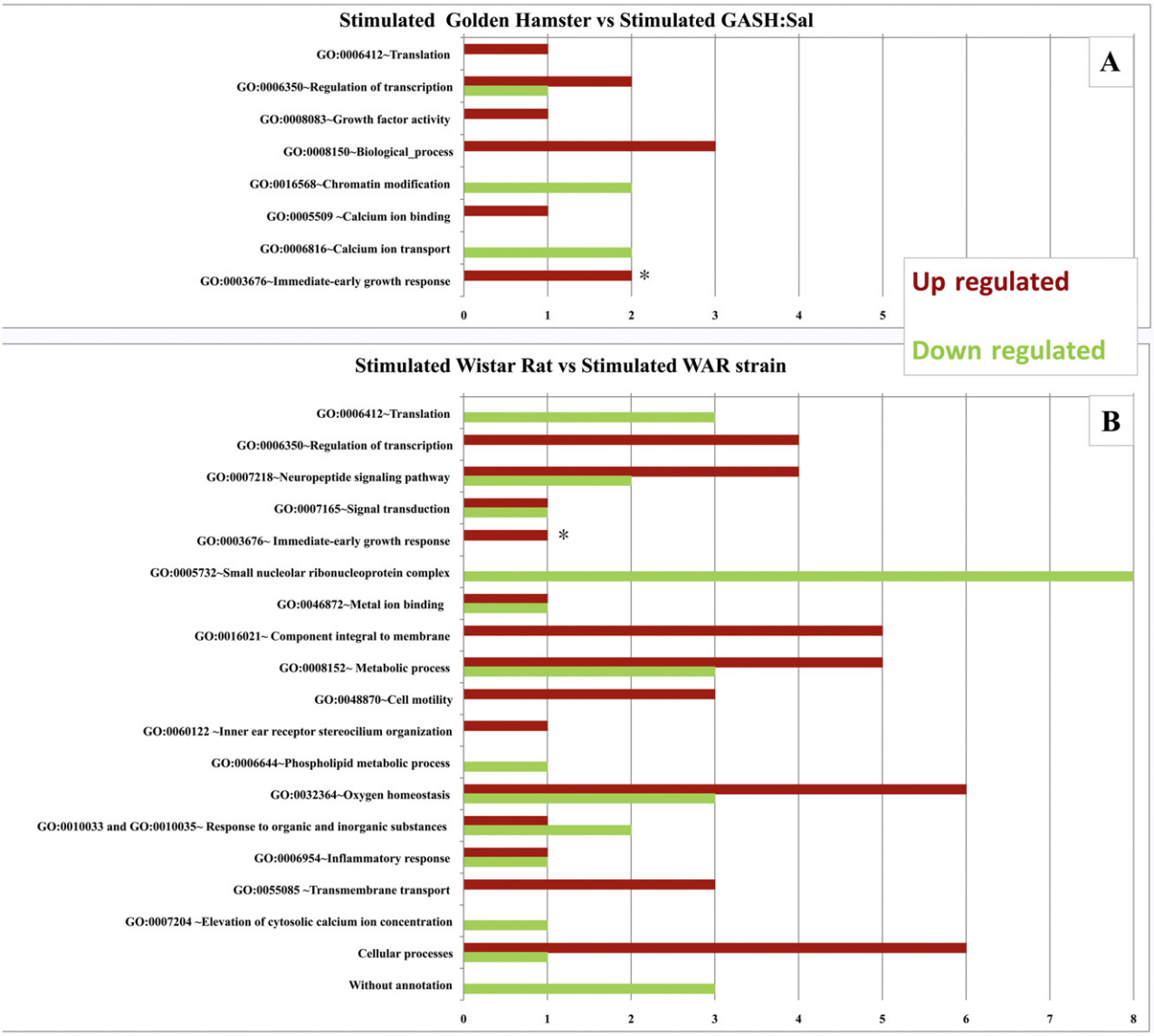

Fig. 1. Functional analysis of the genes in the most representative functional categories based on the Gene Ontology (GO) annotation. The bar graph shows the number of genes up- and downregulated in the IC after sound stimulation in the GASH:Sal (A) and WAR (B) models relative to their respective controls subjected to the same experimental conditions.

annotations (Fig. 1B). Our results indicated that although there were many overrepresented biological function categories, the majority of genes were related to a few function categories. We found certain functions that only corresponded to upregulated genes and other functions that corresponded to only downregulated genes or both up- and downregulated genes (Fig. 1B). In our study, the most relevant function categories included genes involved in responses to different stimuli (epoxide hydrolase 2, cytoplasmic [*Ephx2*], regulator of G-protein signaling 2 [*Rgs2*], regulator of G-protein signaling 5 [*Rgs5*], succinate receptor 1 [*Sucnr1*]), oxygen homeostasis (ATP-binding cassette, subfamily B (MDR/TAP), member 1 [*Abcb1a*], lecithin–cholesterol acyltransferase [*Lcat*], farnesyl diphosphate synthetase [*Fdps*]), metabolic process (DOPA decarboxylase [*Ddc*], phospholysine phosphohistidine inorganic pyrophosphate phosphatase [*Lhpp*], phosphoribosyl pyrophosphate synthetase 1 [*Prps1*], transthyretin [*Ttr*]), translation process (60S ribosomal protein L12 [*LOC499782*]), transcription factors (nitric oxide synthase trafficking [*Nostrin*], polymerase (RNA) III (DNA-directed) polypeptide K [*Polr3k*], SCAN domain-containing *1* [*Scand1*], U2 spliceosomal RNA [*U2*]), neuropeptide signaling pathway (EGF, latrophilin and seven transmembrane domain-containing protein 1 precursor [*ADGRF5*], adhesion G-protein-coupled receptor F5 [*Gpr116*], G-protein-coupled receptor 126 gene [*Gpr126*], 5-hydroxytryptamine receptor 3A [*Htr3a*], neuropeptide Y precursor [*NPY*], tachykinin, precursor 1 [*Tac1*]), calcium metabolism (mitochondrial fission 1 protein [*Fis1*]), and immediate-early growth response (*Egr3*), among other categories (Fig. 1B). Supplemental File 1 shows the complete list of differentially expressed genes.

The comparison between the gene expression profiles of the two seizure animal models using the microarray data showed only one common gene, the *Egr3*, which was upregulated in both cases.

3.2. Quantitative reverse transcription real-time PCR

We performed RT-qPCR analyses to validate the data obtained in the microarrays of the IC corresponding to the sound-stimulated audiogenic strains and their sound-stimulated controls. This included the overexpression of the *Egr3* in the experimental samples compared to the controls for both microarrays used in the present study. Moreover, we checked the expression of other deregulated genes in our microarrays and those belonging to the *Egr* family (*Egr1* and *Egr2*). The results of this set of experiments are shown in Fig. 2 and Table 3.

The three early growth response genes *Egr1*, *Egr2*, and *Egr3* were significantly overexpressed in both stimulated GASH:Sal and WAR compared to their respective stimulated controls (Fig. 2A and B). The value of *Egr3* and *Egr2* expression between stimulated Wistar and WAR rats was extraordinarily high (Fig. 2B), 10 fold higher than that observed for the comparison between stimulated control and GASH:Sal hamsters (Fig. 2A).

Furthermore, we determined the effect of sound stimulation in the IC gene expression, analyzing the expression of the *Egr* genes in the two strains with or without auditory stimulation by RT-qPCR. Thus, the gene expression of the IC in the baseline controls was compared with that in the sound-stimulated audiogenic strains (Fig. 2C and D).

The comparison of gene expression between nonstimulated GASH:Sal and stimulated GASH:Sal indicated that the expression of the three *Egr* genes was significantly higher in the stimulated GASH:Sal (100 fold higher than in the nonstimulated GASH:Sal) (Fig. 2C).

By comparing the nonstimulated WAR with the stimulated WAR, we found that the three *Egr* genes were significantly overexpressed in the stimulated WAR (Fig. 2D). The *Egr1* and *Egr3* expression results were similar to those found in the comparison of the GASH:Sal; alternatively,

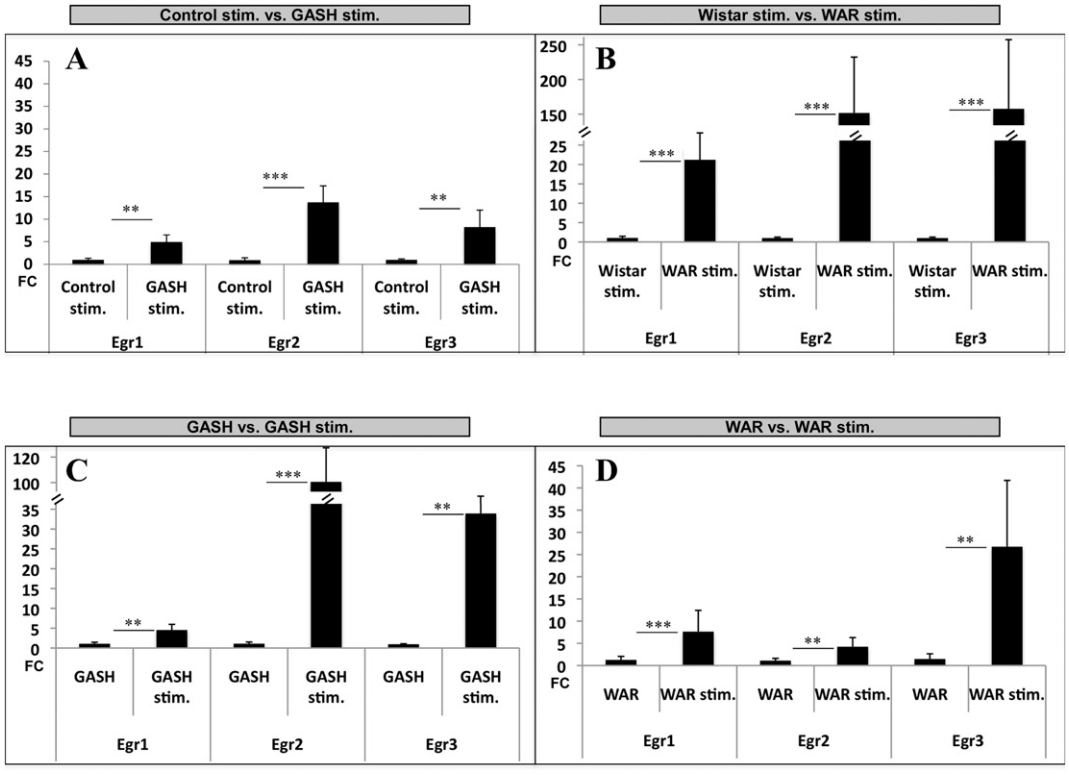

Fig. 2. The fold changes in *Egr* transcript expression in the IC of GASH:Sal and WAR models and their respective controls were measured via RT-qPCR. The expression of the three *Egr* genes was significantly increased in both audiogenic seizure models in comparison to their respective stimulated controls and in comparison with their basal levels. Error bars indicate hemistandard deviation (SD). The housekeeping gene used was β-actin. All the RT-qPCR primers are described in Table 1. Significant differences are indicated as $p < 0.01$ (**) or $p < 0.001$ (***). Abbreviation: FC, fold change (relative mRNA levels).

Table 3
The fold changes in GABRa4 transcript expression in the IC of the GASH:Sal and WAR models and their respective controls were measured via RT-qPCR. In red, upregulated; in green, downregulated. The housekeeping gene used was β-actin. All the RT-qPCR primers are described in Table 1. The significant differences are indicated as $p < 0.001$ (***); NS, not significant ($p > 0.05$).

		Control stim. vs. GASH stim.			GASH vs. GASH stim.		
Gene description	Gene symbol	RT-qPCR		RT-qPCR *p* value	RT-qPCR		RT-qPCR *p* value
		Control stim.	GASH stim.		GASH	GASH stim.	
Gamma-aminobutyric acid (GABA) A receptor α 4 subunit	**GABRa4**	1.02 ± 0.27	0.79 ± 0.20	NS	1.10 ± 0.39	0.94 ± 0.24	NS

		Wistar stim. vs. WAR stim.			WAR vs. WAR stim.		
Gene description	Gene symbol	RT-qPCR		RT-qPCR *p* value	RT-qPCR		RT-qPCR *p* value
		Wistar stim.	WAR stim.		WAR	WAR stim.	
Gamma-aminobutyric acid (GABA) A receptor α 4 subunit	**GABRa4**	1.01 ± 0.19	4.56 ± 1.29	< 0.001 (***)	1.13 ± 0.70	1.42 ± 0.89	NS

Egr2 expression was slightly higher in the stimulated WAR than in the nonstimulated WAR, although not to the extent observed in GASH:Sal.

Finally, we performed RT-qPCR analysis on other genes related to the function of the *Egr3*, such as the gene encoding the gamma-aminobutyric acid (GABA) A receptor, alpha 4 (*GABRa4*), despite not having been detected as deregulated in our microarray analysis. In our study, the expression of the gene encoding the alpha 4 subunit of GABAA receptor was not significantly changed in the IC of the GASH:Sal under any of the conditions studied (Fig. 2A and C). Alternatively, *GABRa4* expression was significantly different in the IC of the sound-stimulated WAR compared to the sound-stimulated controls (Table 3).

3.3. Immunohistochemistry

Since *Egr3* was upregulated in the IC of both audiogenic strains, we studied the distribution of the Egr3 protein in the nervous system under basal conditions and after sound stimulation. Using immunohistochemistry to detect Egr3, we found a similar immunostaining pattern between the two species (Figs. 3 and 4). Early growth response 3 immunopositive neurons were found in the auditory pathway of the stimulated animals and nonstimulated animals. In WAR and GASH:Sal animals, Egr3 immunolabeled neurons were present in all the three divisions of the IC. The majority of Egr3 immunolabeled neurons were found in the dorsal and external cortices of the IC, while weakly stained neurons were found in the central nucleus of the IC (Figs. 3 and 4). Also, Egr3 immunostaining was present in the cochlear nucleus complex (Figs. 3 and 4). Outside the auditory pathway, we found Egr3 immunoreactivity in the hippocampus (Figs. 3 and 4).

Because of the close relationship between *Egr3* expression and the proliferation of B and T lymphocytes [38], we examined the presence of this protein in lymphoma cells sporadically observed in the colony of GASH:Sal [39]. We found immunoreactivity for the Egr3 protein in Burkitt-type non-Hodgkin neoplastic lymphoma tissue, which was previously observed in the GASH:Sal [39]. Early growth response 3 immunostaining revealed focal expression in the lymphoid cells localized to the cytoplasm (Fig. 5).

3.4. Transcriptome comparison

We used the mouse probes for the microarray analyses of gene expression in hamsters as the Syrian hamster probes were not currently available. To confirm these results, we employed Chinese hamster probes (*Cricetulus griseus*) via transcriptomic analysis, comparing the stimulated controls with the stimulated GASH:Sal. The data are available in a database at NCBI under the project number PRJNA230618 (https://submit.ncbi.nlm.nih.gov/ft/byid/bq7rg36z/gashsubmission.sqn). Upon using these probes, the number of differentially expressed genes between stimulated GASH:Sal and the stimulated controls was increased. In the present study, we focused only on the results related to the *Egr* genes. The expression values from RT-qPCR and transcriptomic analyses showed significantly increased values of the early expression genes *Egr1*, *Egr2*, and *Egr3*. In the microarray analysis, we found upregulation of the *Egr2* and *Egr3* genes, but we did not detect upregulation of the *Egr1* (Fig. 6).

4. Discussion

Genetic animal models of epilepsy provide important tools for further understanding the basic cellular mechanisms underlying epileptogenesis and identifying new targets for antiepileptic drugs. They are also used to determine the genetic factors that induce seizures to discover molecular mechanisms in common with human epilepsy.

In the present study, using microarrays, we analyzed the changes in gene expression in two strains with audiogenic epilepsy after a seizure event, compared with controls under the same conditions. The comparison of the gene expression profiles between the two animal models using the microarray data showed only one common gene, *Egr3*, which was upregulated in both cases. On the other hand, using RT-qPCR studies, we confirmed the differential expression of this gene and two other early response genes, *Egr1* and *Egr2*, which were also upregulated in both species. Differences between microarray and RT-qPCR data occur for several reasons, including the fact that different probes are used for the microarray and RT-qPCR experiments (which can capture differential expression in splice variants), differences in the methods for normalization of expression data, and possible false-positive expression changes. In addition, lower correlations between RT-qPCR and microarray results were consistently reported for genes exhibiting small degrees of changes [40].

4.1. Methodological considerations

In our study, the time between the induced seizures and the tissue sampling for the RNA study was 60 min. Since it has been reported that the expression of *Egr2* and *Egr3* is dramatically induced 30 min

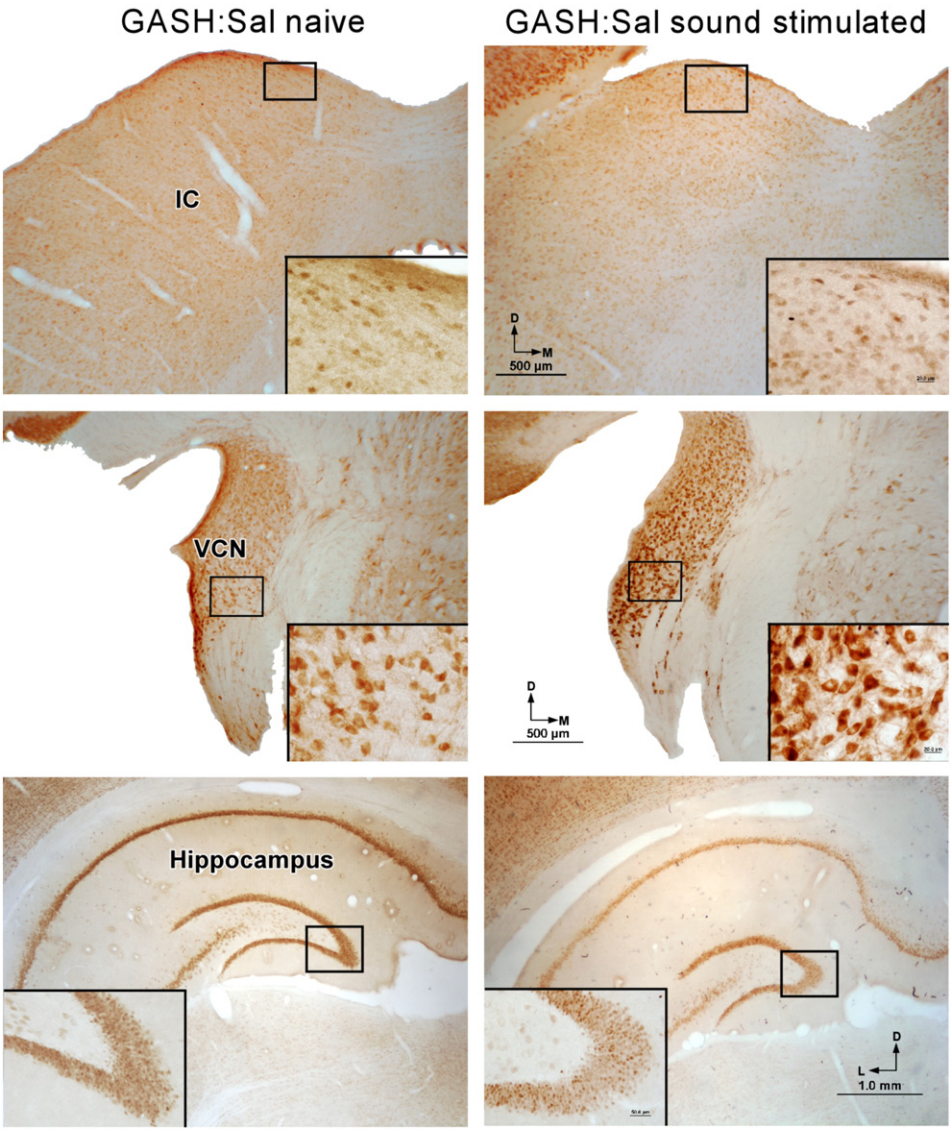

Fig. 3. Coronal sections of GASH:Sal were immunostained to visualize Egr3 protein expression. The inset shows a magnification of the boxed area. Abbreviations: IC, inferior colliculus; VCN, ventral cochlear nucleus.

after the onset of seizures induced by kainic acid [41], we set 60 min as a period of time sufficient to detect *Egr* gene expression. Microarray analysis enables global transcriptomic studies of the changes in gene expression because it enables the simultaneous analysis of thousands of genes in a single experiment. Briefly, after performing the hybridization arrays and after quantitation of the expression level of each probe set in all microarrays, we used a different algorithm to identify probe sets displaying significant differential expression by comparing the samples from audiogenic strains with their respective controls. We selected the genes that varied in a range (fold change) among other genes and used different databases to identify their function. Only genes displaying a $|FC| > 2$ (up- or downregulated) were considered for analysis. For the GASH:Sal, we have chosen a less restrictive criterion, $|FC| > 1.5$, because the probes used were not the most appropriate and did not allow us to detect many changes. Moreover, because a limited number of genes were differentially expressed, few genes fulfilled such a restrictive criterion. On the other hand, we used commercial mouse microarrays to study gene expression in hamsters because the genome of this species has not been described, and therefore, no specific arrays have been developed. Furthermore, it is well known that these two species (*M. auratus* and *Mus musculus*) are phylogenetically very close [42].

Genotyping of *M. auratus* is currently underway at the Broad Institute (NCBI-BioProject accession: PRJNA77669) but is not published yet. Therefore, to confirm the results of our gene expression analysis, we used the cDNA sequences of the Chinese hamster, *C. griseus*, for a comparative analysis of the transcriptomic profiles in the IC from GASH:Sal and control Syrian hamsters, both of which were stimulated with sound. The Chinese hamster genome was recently published [43], and this species displays greater similarity to the Syrian hamster than to the mouse [44].

4.2. Early growth response genes

The *Egr1*, *Egr2*, and *Egr3* genes are immediate-early genes; this term refers to genes whose transcription can be rapidly and transiently induced by a broad range of cellular stimuli (environmental, physiological, and pathological stimuli) [45,46]. These genes encode the EGR family of zinc-finger proteins, which bind to DNA, RNA, or proteins [47,48].

The factors that induce the expression of these genes in mammalian cells include stress [49], which may be induced by chemical and physical external stressors [50] or internal stressors, such as cardiac stress [51], which elevates the *Egr* mRNA level. The increased transcription of *Egr* due to stress occurs in tissues as variant as the adrenal glands [52] and

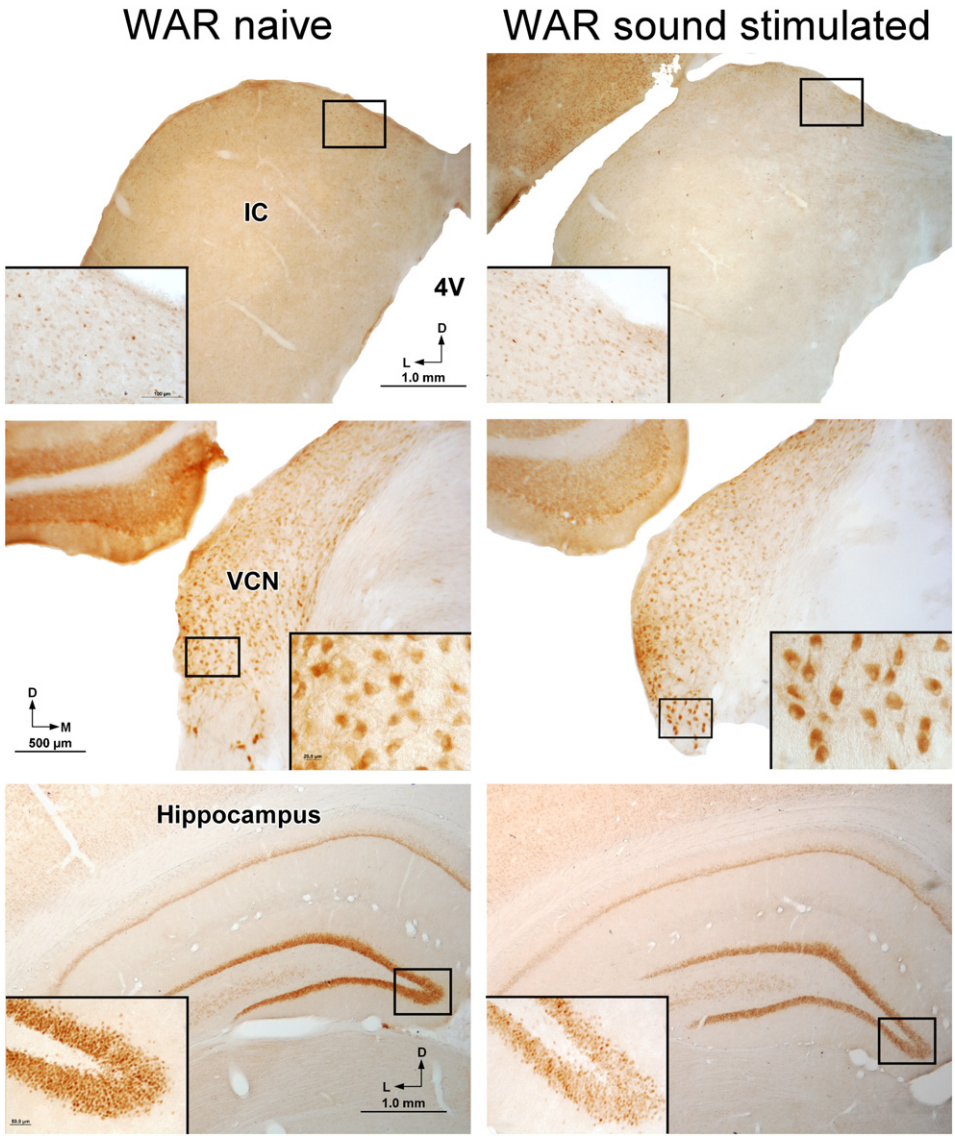

Fig. 4. Coronal sections of WAR were immunostained to visualize Egr3 protein expression. The inset shows a magnification of the boxed area. Abbreviations: 4v, fourth ventricle; IC, inferior colliculus; VCN, ventral cochlear nucleus.

the hippocampus [53]. It has been reported that Egr1 has a clear role in mediating gene expression required for some learning and memory processes [54,55], and Egr3 is associated with neuronal plasticity in response to stress and novelty [56]. In fact, the proteins expressed by the activity-regulated cytoskeletal-related (Arc) gene are directly regulated by *Egr1* and *Egr3*, which can indirectly modulate synaptic plasticity by directly regulating Arc [57].

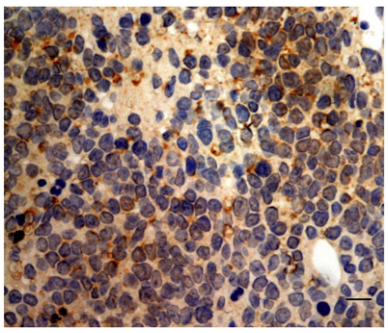

Fig. 5. Egr3 immunopositivity in lymphoid cells of GASH:Sal lymphoma tissue. Scale bar, 10 μm.

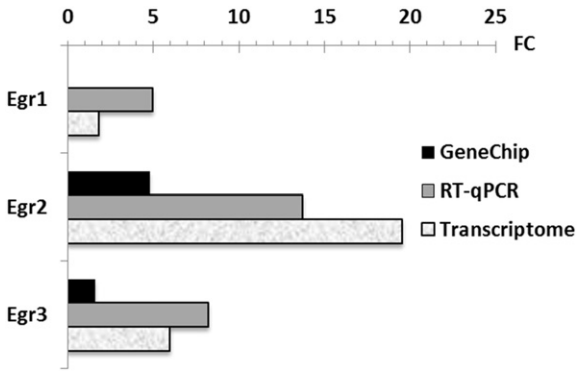

Fig. 6. Confirmation of the results for selected genes at the gene expression level. The fold changes in the expression levels of the three Egr transcripts in the IC of the sound-stimulated GASH:Sal compared to the sound-stimulated Syrian hamster controls were obtained by microarray, RT-qPCR, and transcriptomic analyses. Abbreviations: FC, fold change (relative mRNA levels).

The early growth response genes *Egr1*, *Egr2*, and *Egr3* mediate adaptation to novel stimuli and novelty [58]. This result from our material would explain their presence in the auditory nuclei, where cells respond to the sound. Exposure to novelty resulted in long-term depression (LTD), and *Egr3* has been associated with LTD processes [56], which are also mediated by the serum factor response (*SRF*) gene [59]; this gene was overexpressed in the GASH:Sal transcriptome (data not shown). Mice knocked out for this gene ($Egr3^{-/-}$) show abnormal adaptation to novelty and stress, deficits in startle habituation, and deficits in synaptic plasticity [56]. Based on immunohistochemistry, we found this protein in the hippocampus of WAR and GASH:Sal, in both animals subjected to auditory stimulation and naïve animals. Although we have not quantified the levels of this protein, it does not appear that its expression is increased in the hippocampus of the stimulated animals, and such a result would support its function. However, because the brains were collected 60 min after audiogenic stimulation, it is possible that insufficient time or number of stimulations was responsible for the inability to detect Egr3-immunolabeled differences in the hippocampus.

Different processes that contribute to neuronal hyperexcitability, such as the hyperexcitability produced by ethanol withdrawal [60] and induced seizures [61], resulted in overexpression of these *Egr* genes. Following seizures induced by kainic acid, it was possible to detect the expression pattern of these immediate-early genes (IEGs), especially in the hippocampus, the cortex, and the amygdala [61]. It has been previously reported that the *Egr3* expression is increased in the hippocampus of humans with temporal lobe epilepsy as well as in animal models of temporal lobe epilepsy [62]. On the contrary, Lgi1L385R/+ rats, which showed generalized tonic–clonic seizures in response to acoustic stimuli, have the opposite effect — a downregulation of *Egr2* after sound stimulation [63]. In humans, it has been reported as a common pattern of persistent gene activation in neocortical epileptic foci, including the *Egr1* and the *Egr2* [64] but not the *Egr3*. As far as we know, up to the present, there is no information in the literature regarding the upregulation of these genes and the increment of the corresponding proteins in the IC after the audiogenic seizures in animal models.

Sustained IEG expression might represent either a stress response by which the neurons are trying to protect themselves or an early indicator that these cells are initiating a pathway leading to programmed cell death. In our case, the overexpression of *Egr3* following stimulation in both the WAR and GASH:Sal models could be explained by the essential role of *Egr3* in regulating gene expression to promote fusimotor innervation homeostasis [65], which changes with increased motor activity, as observed for ictal events. Along these lines, it has recently been reported that *Egr3* is a target of critical cocaine-mediated signaling pathways, which are responsible for the induction of locomotor activity [66].

The early growth response 3 gene has also been associated with changes in *GABRa4* expression after status epilepticus [67]. This gene encodes a subunit of the GABAA receptor, an ion channel that mediates the majority of inhibition in the central nervous system. Seizure induced transcriptional upregulation of the α4 subunit gene (*GABRa4*) of this receptor [68] may play an important role in the etiology of temporal lobe epilepsy [67]. In our study, we have found this correlation only in the IC of WAR, which displayed upregulation of the *GABRa4* gene after the ictal event but not in that of GASH:Sal. Perhaps, in the latter model of epilepsy, excitotoxic mechanisms were unrelated to modifications of the expression of the α4 subunit of the GABA receptor but rather were related to modifications in the expression of other subunits (β2) of this receptor, resulting in its dysfunction [69].

Another feature attributable to Egr genes, specifically *Egr3*, is that they play an essential role in the conversion of mitogenic signals by epidermal growth factor into a proliferative response to regulate sympathetic neuronal dendrite morphology and terminal axon branching; these processes are essential for normal sympathetic nervous system development [70]. Together with *Egr2*, Egr3 performs critical functions in the myelination of the peripheral nervous system (Fig. 7) [71].

These transcription factors (*Egr2* and *Egr3*) are also involved in the control of inflammation [67] and in the proliferation of B and T lymphocytes [38,72,73]. Interestingly, we found immunoreactivity for the Egr3 protein in Burkitt-type non-Hodgkin neoplastic lymphoma cells, which were previously observed in the GASH:Sal and in human Burkitt-type B lymphoma [39]. Early growth response 3 is also highly overexpressed in other types of cancer, such as prostate cancer [74] or breast cancer [75]. This relationship between *Egr3* and cancer has not been found for other *Egr* genes, for which the opposite relationship was described. For instance, numerous studies have detailed the

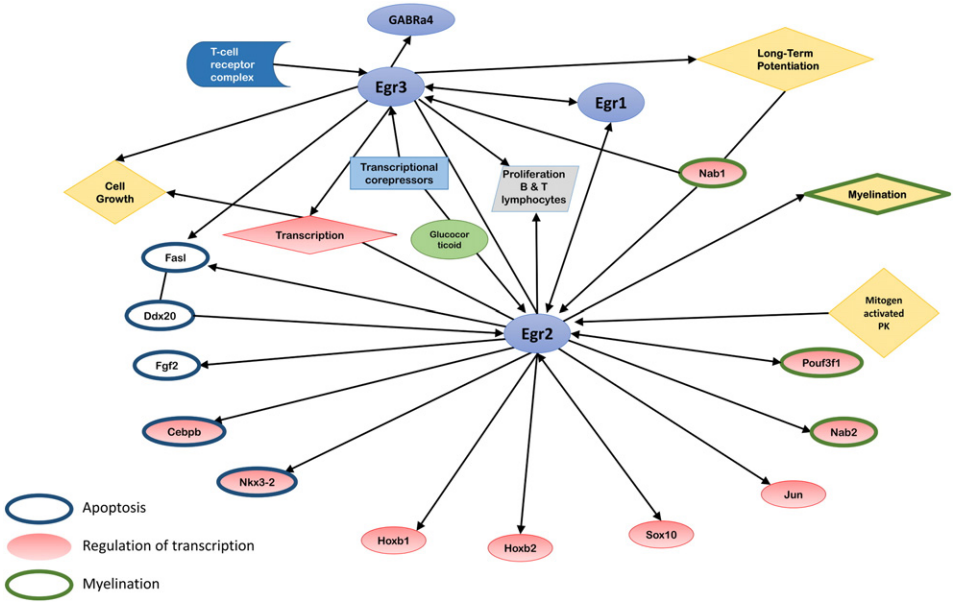

Fig. 7. Schematic relationship between the three Egr genes that were upregulated in the inferior colliculus after audiogenic stimulation in the WAR and GASH:Sal audiogenic seizure models. This figure summarizes the relationship between *Egr* genes associated with processes of cell growth, apoptosis, LTD, corticosteroid signaling, myelination, and transcriptional regulatory genes. These interconnections indicate that Egr proteins act as nuclear effectors of different signals.

tumor suppressor functions of *Egr1* and, consequently, its downregulation in breast, lung, and glial cancers [76–78]. In the near future, we plan to perform further research to determine whether Egr3 can serve as a predictive marker of lymphoma and other cancer types.

5. Conclusions

Ictal events in strains susceptible to audiogenic seizures, specifically WAR and GASH:Sal, cause gene deregulation in the IC.

The technical limitations of the microarray analyses require the validation of the microarray data with real-time RT-PCR. The WAR and GASH:Sal exhibited overexpression of the early growth response genes *Egr1*, *Egr2*, and *Egr3*, presumably as an effect of the stress associated with seizures. The overexpression of these genes was higher in the WAR model than in the GASH:Sal model. These genes are transcription factors, and their activation precedes further transcriptional responses related to myelination processes, cell growth, apoptosis, LTD, and activation of transcriptional regulatory genes. Fig. 7 and Supplemental File 2 summarize the relationship between the *Egr* genes that were upregulated after an ictal event in the two models of audiogenic epilepsy studied, as well as their interconnection with other genes and cellular processes.

The present study showed for the first time upregulation of the early growth response genes *Egr1*, *Egr2*, and *Egr3* in the inferior colliculus (an epileptogenic focus) of the WAR and GASH:Sal strains.

Supplementary data to this article can be found online at http://dx.doi.org/10.1016/j.yebeh.2015.12.020.

Acknowledgments

This study was supported by the Spanish JCyL (#SA023A12-2), University of Salamanca Research Support Grant 2015 (#P1) (to Dr. Dolores E. López), USP/USAL Program for the Promotion of the Bilateral Cooperation in the Field of Research (#2011.1.23386.1.3), USP/USAL (2011.1.23386.81.3), and FAPESP (07/50261-4) (to Norberto Garcia-Cairasco). Norberto Garcia-Cairasco holds a CNPq research fellowship.

Conflict of interest

The authors declare no conflict of interest.

References

[1] Garcia-Cairasco N. Puzzling challenges in contemporary neuroscience: insights from complexity and emergence in epileptogenic circuits. Epilepsy Behav 2009;14(Suppl. 1):54–63.
[2] Garcia-Cairasco N. Learning about brain physiology and complexity from the study of the epilepsies. Braz J Med Biol Res 2009;42:76–86.
[3] Tejada J, Costa KM, Bertti P, Garcia-Cairasco N. The epilepsies: complex challenges needing complex solutions. Epilepsy Behav 2013;26:212–28.
[4] Fisher L, Chaban G, Hertz E. Abnormal metabolic response to excess potassium in astrocytes from the Jimpy mouse, a convulsing neurological mutant. Brain Res 1980; 181:482–7.
[5] Fisher RS. Animal models of the epilepsies. Brain Res Rev 1989;14:245–78.
[6] Case M, Soltesz I. Computational modeling of epilepsy. Epilepsia 2011;52:12–5.
[7] Engel J. Concepts of epilepsy. Epilepsia 1995;36(Suppl. 1):S23–9.
[8] Kandratavicius L, Balista PA, Lopes-Aguiar C, Ruggiero RN, Umeoka EH, Garcia-Cairasco N, et al. Animal models of epilepsy: use and limitations. Neuropsychiatr Dis Treat 2014;10:1693–705.
[9] Serikawa T, Mashimo T, Kuramoto T, Voigt B, Ohno Y, Sasa M. Advances on genetic rat models of epilepsy. Exp Anim 2015;64(1):1–17.
[10] Garcia-Cairasco N, Wakamatsu H, Oliveira JAC, Gomes ELT, Del Bel EA, Mello LEAM. Neuroethological and morphological (Neo-Timm staining) correlates of limbic recruitment during the development of audiogenic kindling in seizure susceptible Wistar rats. Epilepsy Res 1996;26:177–92.
[11] Doretto MC, Fonseca CG, Lobo RB, Terra VC, Oliveira JA, Garcia-Cairasco N. Quantitative study of the response to genetic selection of the Wistar audiogenic rat strain (WAR). Behav Genet 2003;33(1):33–42.
[12] Carballosa-Gonzalez MM, Muñoz LJ, Sancho C, López-Alburquerque T, Pardal-Fernández MJ, Nava E, et al. EEG characterization of audiogenic seizures in the hamster strain GASH:Sal. Epilepsy Res 2013;106:318–25.
[13] Muñoz LJ, Carballosa-Gautam MM, Yanowsky K, García-Atarés N, López DE. The GASH:Sal. Where do we stand and where we're going. Epilepsy Behav 2016 [in press].
[14] Willott JF, Lu SM. Midbrain pathways of audiogenic seizures in DBA/2 mice. Exp Neurol 1980;70(2):288–99.
[15] Ross KC, Coleman JR. Developmental and genetic audiogenic seizure models: behavior and biological substrates. Neurosci Biobehav Rev 2000;24(6):639–53.
[16] Faingold CL. Emergent properties of CNS neuronal networks as targets for pharmacology: application to anticonvulsant drug action. Prog Neurobiol 2004;72(1): 55–85.
[17] Garcia-Cairasco N, Terra VC, Doretto MC. Midbrain substrates of audiogenic seizures in rats. Behav Brain Res 1993;58(1–2):57–67.
[18] Garcia-Cairasco N, Sabbatini RM. Possible interaction between the inferior colliculus and the substantia nigra in audiogenic seizures in Wistar rats. Physiol Behav 1991; 50(2):421–7.
[19] Kesner RP. Subcortical mechanisms of audiogenic seizures. Exp Neurol 1966;15(2): 192–205.
[20] Wada JA, Terao A, White B, Jung E. Inferior colliculus lesion and audiogenic seizure susceptibility. Exp Neurol 1970;28(2):326–32.
[21] Ross KC, Coleman JR. Audiogenic seizures in the developmentally primed Long–Evans rat. Dev Psychobiol 1999;34(4):303–13.
[22] Barrera-Bailón B, Oliveira JAC, López DE, Muñoz LJ, Garcia-Cairasco N, Sancho C. Pharmacological and neuroethological study of three antiepileptic drugs in the genetic audiogenic seizure hamster (GASH:Sal). Epilepsy Behav 2013;28(3):413–25.
[23] Fuentes-Santamaría V, Cantos R, Alvarado JC, García-Atarés N, López DE. Morphological and neurochemical abnormalities in the auditory brainstem of the genetically epilepsy-prone hamster (GPG/Vall). Epilepsia 2005;46(7):1027–46.
[24] Gómez-Nieto R, Rubio ME, López DE. Cholinergic input from the ventral nucleus of the trapezoid body to cochlear nucleus of the trapezoid to cochlear root neurons in rats. J Comp Neurol 2008;506:452–68.
[25] Irizarry RA, Hobbs B, Collin F, Beazer-Barclay YD, Antonellis KJ, Scherf U, et al. Exploration, normalization, and summaries of high density oligonucleotide array probe level data. Biostatistics 2003;4(2):249–64.
[26] Li C, Wong WH. Model-based analysis of oligonucleotide arrays: expression index computation and outlier detection. Proc Natl Acad Sci U S A 2001;98(1):31–6.
[27] Bolstad BM, Irizarry RA, Astrand M, Speed TP. A comparison of normalization methods for high density oligonucleotide array data based on variance and bias. Bioinformatics 2003;19(2):185–93.
[28] Irizarry RA, Bolstad BM, Collin F, Cope LM, Hobbs B, Speed TP. Summaries of Affymetrix GeneChip probe level data. Nucleic Acids Res 2003;31(4):e15.
[29] Barash Y, Dehan E, Krupsky M, Franklin W, Geraci M, Friedman N, et al. Comparative analysis of algorithms for signal quantitation from oligonucleotide microarrays. Bioinformatics 2004;20(6):839–46.
[30] Tusher VG, Tibshirani R, Chu G. Significance analysis of microarrays applied to the ionizing radiation response. Proc Natl Acad Sci U S A 2001;98(9):5116–21.
[31] Benjamini Y, Drai D, Elmer G, Kafkafi N, Golani I. Controlling the false discovery rate in behavior genetics research. Behav Brain Res 2001;125(1–2):279–84.
[32] Storey JD, Tibshirani R. Statistical significance for genome wide studies. Proc Natl Acad Sci U S A 2003;100(16):9440–5.
[33] Edgar R, Domrachev M, Lash AE. Gene Expression Omnibus: NCBI gene expression and hybridization array data repository. Nucleic Acids Res 2002;30:207–10.
[34] Huang da W, Sherman BT, Lempicki RA. Systematic and integrative analysis of large gene lists using DAVID bioinformatics resources. Nat Protoc 2009;4(1):44–57.
[35] Andersen CL, Jensen JL, Orntoft TF. Normalization of real-time quantitative reverse transcription-PCR data: a model-based variance estimation approach to identify genes suited for normalization, applied to bladder and colon cancer data sets. Cancer Res 2004;64(15):5245–50.
[36] Schmittgen TD, Livak KJ. Analyzing real-time PCR data by the comparative C(T) method. Nat Protoc 2008;3(6):1101–8.
[37] Burns MJ, Nixon GJ, Foy CA, Harris N. Standardisation of data from real-time quantitative PCR methods — evaluation of outliers and comparison of calibration curves. BMC Biotechnol 2005;5:31.
[38] Li S, Miao T, Sebastian M, Bhullar P, Ghaffari E, Liu M, et al. The transcription factors Egr2 and Egr3 are essential for the control of inflammation and antigen-induced proliferation of B and T cells. Immunity 2012;37(4):685–96.
[39] Muñoz LJ, Ludeña D, Gedvilaite A, Zvirbliene A, Jandrig B, Voronkova T, et al. Lymphoma outbreak in the hamster GASH:Sal strain. Arch Virol 2013;150:2255–65.
[40] Morey JS, Ryan JC, Van Dolah FM. Microarray validation: factors influencing correlation between oligonucleotide microarrays and real-time PCR. Biol Proced Online 2006;8:175–93.
[41] Honkaniemi J, Sharp FR. Prolonged expression of zinc finger immediate-early gene mRNAs and decreased protein synthesis following kainic acid induced seizures. J Neurosci 1999;11(1):10–7.
[42] Fabre PH, Hautier L, Dimitar Dimitrov D, Douzery EJP. A glimpse on the pattern of rodent diversification: a phylogenetic approach. BMC Evol Biol 2012;12:88.
[43] Lewis NE, Liu X, Li Y, Nagarajan H, Yerganian G, O'Brien E, et al. Genomic landscapes of Chinese hamster ovary cell lines as revealed by the *Cricetulus griseus* draft genome. Nat Biotechnol 2013;31(8):759–65.
[44] Tchitchek N, Safronetz D, Rasmussen AL, Martens C, Virtaneva K, Porcella SF, et al. Sequencing, annotation and analysis of the Syrian hamster (*Mesocricetus auratus*) transcriptome. PLoS One 2014;9(11):e112617.
[45] Beckmann MA, Wilce PA. Egr transcription factors in the nervous system. Neurochem Int 1997;31:477–510.
[46] Patwardhan S, Gashler A, Siegel MG, Chang LC, Joseph LJ, Shows TB, et al. EGR3, a novel member of the Egr family of genes encoding immediate-early transcription factors. Oncogene 1991;6:917–28.

[47] Crosby SD, Puetz JJ, Simburger KS, Fahrner TJ, Milbrandt J. The early response gene NGFI-C encodes a zinc finger transcriptional activator and is a member of the GCGGGGGCG (GSG) element-binding protein family. Mol Cell Biol 1991;11:3835–41.
[48] O'Donovan KJ, Tourtellotte WG, Millbrandt J, Baraban JM. The EGR family of transcription-regulatory factors: progress at the interface of molecular and systems neuroscience. Trends Neurosci 1999;22:167–73.
[49] Senba E, Ueyama T. Stress-induced expression of immediate early genes in the brain and peripheral organs of the rat. Neurosci Res 1997;29(3):183–207.
[50] Ronkina N, Menon MB, Schwermann J, Arthur JSC, Legault H, Telliez J-B, et al. Stress induced gene expression: a direct role for MAPKAP kinases in transcriptional activation of immediate early genes. Nucleic Acids Res 2011;39(7):2503–18.
[51] Shieh JTC, Huang Y, Gilmore J, Srivastava D. Elevated miR-499 levels blunt the cardiac stress response. PLoS One 2011;6(5):e19481.
[52] Honkaniemi J, Zhang JS, Longo FM, Sharp FR. Stress induces zinc finger immediate early genes in the rat adrenal gland. Brain Res 2000;877(2):203–8.
[53] Honkaniemi J, States BA, Weinstein PR, Espinoza J, Sharp FR. Global ischemia induces immediate early genes encoding zinc finger transcription factors. J Cereb Blood Flow Metab 1997;17:636–46.
[54] Abraham WC, Dragunow M, Tate WP. The role of immediate early genes in the stabilization of long-term potentiation. Mol Neurobiol 1991;5:297–314.
[55] Worley PF, Bhat RV, Baraban JM, Erickson CA, McNaughton BL, Barnes CA. Thresholds for synaptic activation of transcription factors in hippocampus: correlation with long-term enhancement. J Neurosci 1993;13:4776–86.
[56] Gallitano-Mendel A, Izumi Y, Tokuda K, Zorumski CF, Howell MP, Muglia LJ, et al. The immediate early gene early growth response gene 3 mediates adaptation to stress and novelty. Neuroscience 2007;148:633–43.
[57] Li L, Carter J, Gao X, Whitehead J, Tourtellotte WG. The neuroplasticity-associated arc gene is a direct transcriptional target of early growth response (Egr) transcription factors. Mol Cell Biol 2005;25(23):10286–300.
[58] Poirier R, Cheval H, Mailhes C, Garel S, Charnay P, Davis S, et al. Distinct functions of Egr gene family members in cognitive processes. Front Neurosci 2008;2(1):47–55.
[59] Lindecke A, Korte M, Zagrebelsky M, Horejschi V, Elvers M, Widera D, et al. Long-term depression activates transcription of immediate early transcription factor genes: involvement of serum response factor. Eur J Neurosci 2006;24:555–63.
[60] Beckmann AM, Matsumoto I, Wilce PA. AP-1 and Egr DNA-binding activities are increased in rat brain during ethanol withdrawal. J Neurochem 1997;69(1):306–14.
[61] Honkaniemi J, Sharp FR. Prolonged expression of zinc finger immediate-early gene mRNAs and decreased protein synthesis following kainic acid induced seizures. Eur J Neurosci 1999;11(1):10–7.
[62] Roberts DS, Hu Y, Lund IV, Brooks-Kayal AR, Russek SJ. Brain-derived neurotrophic factor (BDNF)-induced synthesis of early growth response factor 3 (Egr3) controls the levels of type A GABA receptor α 4 subunits in hippocampal neurons. J Biol Chem 2006;281(40):29431–5.
[63] Fumoto N, Mashimo T, Masui A, Ishida S, Mizuguchi Y, Minamimoto S, et al. Evaluation of seizure foci and genes in the Lgi1(L385R/+) mutant rat. Neurosci Res 2014;80:69–75.
[64] Rakhade SN, Yao B, Ahmed S, Asano E, Beaumont TL, Shah AK, et al. A common pattern of persistent gene activation in human neocortical epileptic foci. Ann Neurol 2005;58:736–47.
[65] Fernandes OM, Tourtellotte WG. Egr3-dependent muscle spindle stretch receptor intrafusal muscle fiber differentiation and fusimotor innervation homeostasis. J Neurosci 2015;35(14):5566–78.
[66] Chandra R, Francis TC, Konkalmatt P, Amgalan A, Gancarz AM, Dietz DM, et al. Opposing role for Egr3 in nucleus accumbens cell subtypes in cocaine action. J Neurosci 2015;35(20):7927–37.
[67] Grabenstatter HL, Russek SJ, Brooks-Kayal AR. Molecular pathways controlling inhibitory receptor expression. Epilepsia 2012;53(Suppl. 9):71–8.
[68] Roberts DS, Raol YH, Bandyopadhyay S, Lund IV, Budreck EC, Passini MJ, et al. Egr3 stimulation of GABRA4 promoter activity as a mechanism for seizure-induced up-regulation of GABAA receptor α4 subunit expression. Proc Natl Acad Sci U S A 2005;102(33):11894–9.
[69] Prieto-Martín AI, Aroca-Aguilar JD, Sánchez-Sánchez F, Muñoz LJ, López DE, Escribano J, et al. Molecular and neurochemical substrates of the audiogenic seizure strains: the GASH:Sal model. Epilepsy Behav 2017;71:218–25.
[70] Quach DH, Oliveira-Fernandes M, Gruner KA, Tourtellotte WG. A sympathetic neuron autonomous role for Egr3-mediated gene regulation in dendrite morphogenesis and target tissue innervation. J Neurosci 2013;33(10):4570–83.
[71] Tourtellotte WG, Milbrandt J. Sensory ataxia and muscle spindle agenesis in mice lacking the transcription factor Egr3. Nat Genet 1998;20:87–91.
[72] Sumitomo S, Fujio K, Okamura T, Yamamoto K. Egr2 and Egr3 are the unique regulators for systemic autoimmunity. JAKSTAT 2013;2(2), e23952.
[73] Lazarevic V, Zullo AJ, Schweitzer MN, Staton TL, Gallo EM, Crabtree GR, et al. The gene encoding early growth response 2, a target of the transcription factor NFAT, is required for the development and maturation of natural killer T cells. Nat Immunol 2009;10:306–13.
[74] Pio R, Jia Z, Baron VT, Mercola D. Early growth response 3 (Egr3) is highly overexpressed in non-relapsing prostate cancer but not in relapsing prostate cancer. PLoS One 2013;8(1):e54096.
[75] Inoue A, Omoto Y, Yamaguchi Y, Kiyama R, Hayashi SI. Transcription factor EGR3 is involved in the estrogen-signaling pathway in breast cancer cells. J Mol Endocrinol 2004;32:649–61.
[76] Levin WJ, Casey G, Ramos JC, Arboleda MJ, Reissmann PT, Slamon DJ. Tumor suppressor and immediate early transcription factor genes in non-small cell lung cancer. Chest 1994;106:372S–6S.
[77] Huang RP, Liu C, Fan Y, Mercola D, Adamson ED. Egr-1 negatively regulates human tumor cell growth via the DNA-binding domain. Cancer Res 1995;55:5054–62.
[78] Calogero A, Arcella A, De Gregorio G, Porcellini A, Mercola D, Liu C, et al. The early growth response gene EGR-1 behaves as a suppressor gene that is down-regulated independent of ARF/Mdm2 but not p53 alterations in fresh human gliomas. Clin Cancer Res 2001;7:2788–96.